Economic Value of Energy Storage Systems: The Influence of Ownership Structures

Nan Gu, *Graduate Student Member, IEEE*, Chenye Wu, *Senior Member, IEEE*, and Daniel S. Kirschen, *Fellow, IEEE*

***Abstract*—Owners of renewable energy resources (RES) often choose to invest in energy storage for joint operation with RES to maximize profitability. Standalone entities also invest in energy storage systems and use them for arbitrage. In this paper we examine how these two forms of ownership affect the value of energy storage. Our study reveals that in a perfectly competitive market, energy storage holds equal value for both types of owners if they are risk-neutral. However, when agents are able to exert market power or exhibit risk aversion, the value of energy storage can differ between the two ownership structures. Additionally, we discuss how differential pricing and market barriers influence the value of energy storage. In the numerical studies, we explore how factors such as seasonal price volatility, RES types, and the siting of energy storage influence investment decisions.**

***Index Terms*—Energy storage, ownership, renewable energy resources, risk preferences.**

NOMENCLATURE

Results

Π^*_{Joint}	Optimal aggregated profits of joint operation.
Π^*_{ORI}	Original optimal profit of the RES generator before the integration of the energy storage.
Π^*_{RES}	Optimal profits for RES generator in the disjoint operation mode.
Π^*_{Storage}	Optimal profits for energy storage arbitrageur in the disjoint operation mode.
$\Pi_{\text{Joint}_{\text{Mono}}}$	Optimal profits of joint operation with "Sell-only" restriction.

Indexes, Symbols, and Functions

$\dagger$	Symbol for transposition.
$\Omega(\cdot)$	Feasible region of the real-time decision variables (with different superscripts).
$\rho[\cdot]$	General risk measure function.
Θ	General representation of the uncertainty set.
θ	General representation for uncertain variables.
F_Π	Cumulative distribution function of Π.
K	Number of real-time regulation service calls during a market clearing interval.
T	Number of time periods in the optimization horizon.

Parameters

α_w	Risk-averse level of RES owner.
α_x	Risk-averse level of storage arbitrageur.
$\bar{S}$	Capacity of energy storage.
$\bar{w}_t$	Available output of RES during time t in the deterministic model.
$\boldsymbol{\mathcal{P}}$	Uncertainty set of real-time price.
$\boldsymbol{\mathcal{W}}_t$	Uncertainty set of RES output realization.
$\widetilde{\boldsymbol{p}}^{\mathbf{R}}$	Vector form for uncertain real-time energy price.
$\boldsymbol{p}$	Vector form for determistic energy price.
$\boldsymbol{p}^{\mathbf{D}}$	Vector form for day-ahead energy price.
$\boldsymbol{p}^{\boldsymbol{L}}$	Price per unit for down-regulation capacity.
$\boldsymbol{p}^{\boldsymbol{U}}$	Price per unit for up-regulation capacity.
η_c	Charging efficiency of energy storage.
η_d	Discharging efficiency of energy storage.
$\widetilde{\mathbf{w}}$	Vector form for uncertain realizable output of the RES.
$\widetilde{\tau}^L_{t,k}$	Uncertain proportion of down-regulation capacity deployed at time t, interval k.
$\widetilde{\tau}^U_{t,k}$	Uncertain proportion of down-regulation capacity deployed at time t, interval k.
$\widetilde{p}^R_t$	Uncertain real-time energy price during time t.
$\widetilde{w}_t$	Uncertain realizable output of the RES.
L	Maximum ramp capacity of energy storage.
p_t	Determistic Energy price during time t.
p^D_t	Day-ahead Energy price during time t.

Superscripts Associated with Variables

D	Day-ahead market.
F	Aggregate impact of day-ahead and real-time decisions on energy storage operation.
R	Real-time market.

Variables

$\boldsymbol{r}^{\mathbf{L}}$	Vector form for day-ahead down-regulation bids.
$\boldsymbol{r}^{\mathbf{U}}$	Vector form for day-ahead up-regulation bids.
$\boldsymbol{w}$	Vector form for quantity of energy sold by the RES.

Manuscript received 14 July 2023; revised 21 November 2023; accepted 27 December 2023. Date of publication 2 January 2024; date of current version 13 September 2024. This work was supported in part by the National Natural Science Foundation of China under Grant 72271213, and in part by Shenzhen Science and Technology Program under Grants JCYJ20220530143800001, RCYX20221008092927070, and ZDSYS20220606100601002. Paper no. TEMPR-00126-2023. *(Corresponding author: Chenye Wu.)*

Nan Gu was with the University of Washington, Seattle, WA 98195 USA. She is now with the Institute for Interdisciplinary Information Sciences, Tsinghua University, Beijing 100084, China (e-mail: gn19@mails.tsinghua.edu.cn).

Chenye Wu is with the School of Science and Engineering, The Chinese University of Hong Kong, Shenzhen, Guangdong 518172, China (e-mail: chenyewu@yeah.net).

Daniel S. Kirschen is with the Department of Electrical and Computer Engineering, University of Washington, Seattle, WA 98195 USA (e-mail: kirschen@uw.edu).

Digital Object Identifier 10.1109/TEMPR.2023.3349134

$\boldsymbol{x}$	Vector form for the volume of energy traded between the storage system and the grid.
c_t	Amount of energy charged into storage at time t.
d_t	Amount of energy discharged by storage at time t.
r_t^L	Day-ahead bids for down-regulation capacity.
r_t^U	Day-ahead bids for up-regulation capacity.
S_t	State-of-charge (SOC) of the energy storage at time t.
w_t^c	Amount of energy curtailed by the RES at time t.
w_t	Quantity of energy sold by the RES during time t.
x_t	Volume of energy traded between the storage system and the grid at time t.

I. Introduction

AS ESTIMATED by the International Energy Agency [1], the global installed storage capacity will experience a remarkable growth of 56% from 2021, surpassing 270 GW by 2026. Despite the relatively high upfront costs of energy storage, two compelling economic benefits justify its installation. Firstly, energy storage enables independent entities to profit from variations in energy prices through arbitrage. During low energy prices, these entities can purchase electricity from the grid, store it, and sell it at higher prices during peak periods. With the increasing share of renewable energy resources (RES), energy prices exhibit higher volatility, creating additional opportunities for these arbitrageurs to generate profits. Secondly, energy storage gives owners of RES the ability to optimize the sale of their outputs at favorable prices. Storage also helps RES owners reduce or eliminate the penalties incurred when their actual energy generation differs from their ex-ante commitments. The integration of energy storage with RES has been thriving, with 48% of solar capacity and 8% of wind capacity in the U.S. interconnection queue by the end of 2022 being paired with energy storage systems [2]. If the energy storage system is deployed by an entity that also owns RES, we will call its ownership "hybrid", and describe its operation as "joint", or "coordinated" with the renewable generation. On the other hand, if the energy storage system is controlled by an entity that does not own RES, we will label it "independent", or "standalone" and call its operation "disjoint", "separate", or "uncoordinated".

Among the storage projects in the U.S. interconnection queues by the end of 2022, the two ownership structures are about equally distributed: standalone arbitrageurs account for 325 GW of storage capacity, while hybrid plants represent 358 GW of storage capacity [2]. However, standalone storage projects tend to come online faster than hybrid plants [2].

The coexistence of these two types of ownership raises important questions: Do joint hybrid and independent ownership of storage and RES yield equivalent value from energy storage? Are there circumstances where they produce distinct values? This paper aims to provide insights into these questions that have not been comprehensively addressed in the existing literature.

A. Related Works

The abundant literature on the economic value of energy storage for joint operation with renewable generation can be broadly categorized into two distinct groups. The first category emphasizes energy storage's ability to shift renewable generation from low-price periods to high-price periods and proposes strategies to maximize economic benefits, either considering the hybrid plants as price takers [3], [4], or assuming that they are price makers [5], [6]. The second category investigates how energy storage can help owners of renewable generation in mitigating the consequences of forecasting errors. Many of these studies adopt a two-stage model, where the hybrid plant makes commitments to sell at the day-ahead stage, and either pays a penalty or adjusts its bid at the real-time or settlement stage, based on the actual RES output. In some papers, the RES owners are assumed to be risk-neutral [7], [8], [9], while in others they are treated as risk-averse [10], [11]. Additionally, research works such as [12], [13] explore the bidding and operation of hybrid plants using multi-stage and multi-timescale models, offering important context for our discussion. Other studies highlight the arbitrage potential of standalone energy storage systems and examine how storage can leverage fluctuating market prices to maximize economic gains [14], [15]. A third line of research focuses on the potential for storage to maximize profits through arbitrage of the day-ahead and real-time markets [16], [17].

However, a limited amount of research bridges the gap between these research directions to compare the economic value of energy storage under different ownership structures. While a few case studies [5], [7], [8] mention this question, they do not provide a comprehensive theoretical analysis and primarily discuss specific circumstances rather than providing a general framework. For instance, Shioshansi [5] includes the assumption of additional taxes imposed on the wind farm, whereas both [7], [8] assume that the energy price in the second stage can vary for excesses and shortages. These specific assumptions limit the applicability of their findings and highlight the need for a more comprehensive theoretical analysis, which we aim to address in this paper. The most closely related work to our study is [18], where Tercca et al. analytically investigate if there exists economic benefit from jointly operating RES and energy storage under the assumption that both agents are price-takers and risk-neutral. In contrast, our study extends these assumptions to explore scenarios involving price-maker scenarios, risk aversion, two-price settlement conditions, and the participation of energy storage in ancillary markets, thereby offering a comprehensive analysis that reflects more varied and realistic market conditions. It should be noted that our initial analysis targets the economic values in energy markets. Section IV broadens this scope to evaluate energy storage's overall value, encompassing both energy markets and ancillary services such as up and down regulation, with insights from studies in [12], [19], [20], [21].

B. Contributions

The main contributions of this paper are:

1) It provides a comprehensive theoretical comparison of the economic value of energy storage for arbitrageurs and RES

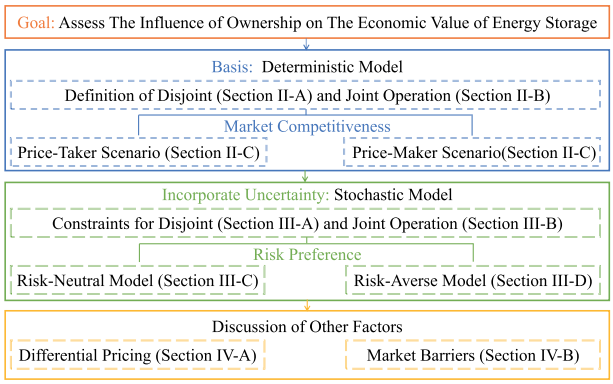

Fig. 1. Structural paradigm of this paper.

owners. Previous work examined this value for only one or the other of these ownership structures.

2) It considers whether these owners are price-takers, price-makers agents, as well as their risk preferences.
3) It discusses how special circumstances may affect which ownership is preferable.
4) A case study provides practical guidance on determining the optimal ownership of a storage asset.

The remainder of this paper is organized as follows. Section II presents a deterministic optimization framework for both ownership structures. Using this framework, we analyze the influence of market competitiveness on the value of storage under both forms of ownership. Section III introduces a two-stage model that incorporates the uncertainty of RES output. This model supports our analysis of the owner's risk preferences on the value of storage. Section IV discusses practical scenarios that deviate from the analysis presented in the previous sections. Section V presents the results of numerical studies. Section VI concludes. Furthermore, Fig. 1 demonstrates the structural paradigm of this paper.

II. Deterministic Model

Without loss of generality, we focus on a system comprising a single RES generator and a newly added energy storage system. The trading timeframe is segmented into distinct, discrete intervals. To highlight the difference between the disjoint and the joint operation, we first adopt a deterministic model i.e., we assume that agents have perfect foresight about the RES output and prices. If this new energy storage is owned by an independent arbitrageur, the two agents operate in the "disjoint" mode, yielding separate profits. On the other hand, if the new energy storage is owned by the RES owner, it is operated in the "joint" mode. The value of energy storage for the RES owner is thus $\Pi^*_{\text{Joint}} - \Pi^*_{\text{ORI}}$, while the value for the independent entity is Π^*_{Storage}.

A. Disjoint Operation

In this mode, the RES is operating on its own as formulated in the optimization problem (1).

$$\max_{\boldsymbol{w}} \ \boldsymbol{p}^\dagger \boldsymbol{w} \tag{1a}$$

$$s.t. \quad w_t = \bar{w}_t - w^c_t, \ \forall t, \tag{1b}$$

$$0 \le w^c_t \le \bar{w}_t, \ \forall t. \tag{1c}$$

Energy curtailment may occur due to non-ideal electricity prices, and Constraint (1c) defines the minimum and maximum limits for this curtailment.

The independent storage owner performs arbitrage according to the optimization problem (2).

$$\max_{\boldsymbol{x}} \ \boldsymbol{p}^\dagger \boldsymbol{x} \tag{2a}$$

$$s.t. \quad x_t = d_t - c_t, \ \forall t, \tag{2b}$$

$$S_{t+1} = S_t - \frac{1}{\eta_d} d_t + \eta_c c_t, \ \forall t, \tag{2c}$$

$$0 \le d_t \le L, \quad 0 \le c_t \le L, \ \forall t, \tag{2d}$$

$$0 \le S_t \le \bar{S}, \ \forall t, \quad S_0 = S_T = \frac{1}{2}\bar{S}. \tag{2e}$$

When the storage system purchases energy from the grid, $x_t < 0$; conversely, if it sells energy to the grid, $x_t \ge 0$. Constraint (2e) forces the state-of-charge (SOC) to return to its initial level at the end of the horizon.

Remark: We set the initial and final states of an energy storage system to half of its capacity for three primary reasons: 1) Pure Arbitrage: This approach ensures that the energy system's profits are generated purely from arbitrage opportunities rather than relying on the energy initially stored in the device. 2) Cyclical Renewal: This method establishes a standard cycle in the system's operations, where each optimization period begins with the same SOC. 3) Reasonable Flexibility: Initiating and concluding with half of the capacity provides the storage system with reasonable flexibility for both charging and discharging during the optimization period.

B. Joint Operation

In the joint operation mode, the energy storage system is integrated with RES to capitalize on the volatility of market prices. For instance, it allows for storing the output of RES during periods of low prices and subsequently selling it when prices reach their highest levels. Problem (3) defines this joint operation.

$$\max_{\boldsymbol{w},\boldsymbol{x}} \ \boldsymbol{p}^\dagger (\boldsymbol{x} + \boldsymbol{w}) \tag{3a}$$

$$s.t. \quad x_t + w_t = \bar{w}_t - w^c_t + d_t - c_t, \forall t, \tag{3b}$$

$$\text{Constraint (1c)}, \tag{3c}$$

$$\text{Constraints (2c)} - \text{(2e)}. \tag{3d}$$

Constraint (3b) states that the energy sold in the market is determined by the sum of the RES output and the net storage discharge and thus couples their operation. This constraint can also be interpreted as a composition of (1b) and (2b), enabling the transfer of energy from the RES generator to the energy storage system. Constraint (3d) the operational constraints on the energy storage system. We provide proof that the current formulation ensures the avoidance of simultaneous charging

and discharging in Appendix B. This formulation of the joint operation mode allows for "two-way" trading, where the RES owner can both sell and purchase energy. As we will discuss in Section IV, some electricity markets do not allow this form of trading.

C. Equivalence Under Price-Taker Scenario

Let us first analyze a perfectly competitive market where none of the agents have market power and all are therefore price-takers. The market price $\boldsymbol{p}$ is then an exogenous variable unaffected by the dispatch decisions of the owners of RES and energy storage. Terça and Wozabal [18] discuss a similar scenario.

Proposition 1: When $\boldsymbol{p}$ is exogenous, the optimum value of the joint problem (3) is the sum of the optimal values of problems (1) and (2), i.e., $\Pi^*_{\text{Joint}} = \Pi^*_{\text{RES}} + \Pi^*_{\text{Storage}}$.

Proof Sketch: Constraint (1b) and (2b) can be regarded as a way of decomposing Constraint (3b) to decouple the decision variables, i.e., $\boldsymbol{x}$ and $\boldsymbol{w}$. Therefore, Problem (3) can be considered the master problem of primal decomposition, and Problems (1) and (2) are the two separate sub-problems. The master problem aims to maximize the sum of the optimal values of the sub-problems over various ways of decomposing the Constraint (3b). It can be proved that Constraint (1b) and Constraint (2b) can achieve the optimality of the master problem, i.e., when Problem (1) and Problem (2) achieve optimality, the optimal solutions given by them correspond to the optimal solution to Problem (3). Appendix A gives the details of the proof.

Since $\boldsymbol{p}$ is an exogenous variable, Π^*_{ORI} is equal to Π^*_{RES}. Proposition 1 thus implies that the value of the energy storage system for an RES owner is equivalent to its value for an independent arbitrageur, i.e., $\Pi^*_{\text{Joint}} - \Pi^*_{\text{ORI}} = \Pi^*_{\text{Storage}}$.

D. Distinction Under Price-Maker Scenario

When the RES generator and energy storage have market power, they are price-makers and their energy offers affect the market-clearing prices. The residual demand curve f [22] relates the prices $\boldsymbol{p}$ and the bids from the price-makers, i.e., $\boldsymbol{p} = f(\boldsymbol{w}, \boldsymbol{x})$. The coupling between $\boldsymbol{x}$ and $\boldsymbol{w}$ is thus more complex than in the price-taker model. In the disjoint mode, each agent acts in its own self-interest, but their respective profits depend on their combined actions. The two optimization problems ((1) and (2)) naturally fall within the framework of non-cooperative game theory. By contrast, the joint operation mode can be framed as a cooperative game, where the RES and energy storage form a coalition to collectively determine joint actions. Fig. 2 illustrates these two modes of operation.

Proposition 2: When $\boldsymbol{p}$ is a function of $\boldsymbol{x}$ and $\boldsymbol{w}$, the optimal value of the joint operation problem (3) is no smaller than the sum of the optimal value of the two separate problems, (1) and (2), i.e., $\Pi^*_{\text{Joint}} \geq \Pi^*_{\text{RES}} + \Pi^*_{\text{Storage}}$.

Proof: Combining Problem (1) and Problem (2) as a single optimization problem, introduces an additional constraint to Problem (3), which leads to a reduction in the feasible set for the combined problem. Since the objective functions are the same, we must therefore have $\Pi^*_{\text{Joint}} \geq \Pi^*_{\text{RES}} + \Pi^*_{\text{Storage}}$.

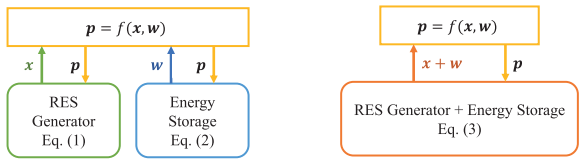

(a) Non-cooperative: Disjoint. (b) Cooperative: Joint.

Fig. 2. Comparison of the two operation modes in the price-maker scenario.

TABLE I
COMPARISON BETWEEN JOINT AND DISJOINT OPERATION IN THE PRICE-MAKER MODEL OF EXAMPLE 1

Stage	Joint Operation		Disjoint Operation		
	$w^* + x^*$ (MWh)	p^* ($/MWh)	w^* (MWh)	x^* (MWh)	p^* ($/MWh)
1	4	11	3	−2	14
2	14	21	15	2	18
Profit	$338		$312 + $8 = $320		

Example 1: To show that Π^*_{Joint} can, at times, be strictly greater than the sum of Π^*_{RES} and Π^*_{Storage}, let us assume a linear residual demand curve where the market-clearing price decreases monotonically with the energy sold by the RES and the storage, i.e., $p_t = \alpha_t - \beta(w_t + x_t)$. In this example, $T = 2$. The decreasing relationship is referred to as the "price-suppressing effect" in [5], which signifies the propensity of sales from renewable energy sources and energy storage to reduce electricity prices. The intercept varies with time, $\alpha_1 = \$15$, $\alpha_2 = \$35$, while the slope $\beta = \$1/\text{MWh}$. The actual output of the RES generator satisfies $\bar{w}_1 = 3\,\text{MWh}$, $\bar{w}_2 = 15\,\text{MWh}$. For the energy storage, it is assumed that $\eta_c = \eta_d = 1$, $L = 5\,\text{MWh}$, and $\bar{S} = 10\,\text{MWh}$.

First, we calculate the Nash Equilibrium when the RES generator and energy storage are owned by separate entities. Since $|x_t| \leq L = 5, \forall t$, we have:

$$\partial \Pi_{\text{RES}}/\partial w_1 = \alpha_1 - \beta x_1 - 2\beta w_1 \geq 15 - 5 - 2 \times 3 = 4,$$

$$\partial \Pi_{\text{RES}}/\partial w_2 = \alpha_2 - \beta x_2 - 2\beta w_2 \geq 35 - 5 - 2 \times 15 = 0,$$

which implies that the profit of RES is monotonically non-decreasing with the energy sold by the RES. Therefore, regardless of the strategy pursued by the storage, the optimal strategy for the RES generator is $w_t = \bar{w}_t$. For the storage's operation, Constraints (2c)–(2e) lead to $x_1 = -x_2$. Considering the opponent's (RES's) strategy, we have:

$$\begin{aligned}\partial \Pi_{\text{Storage}}/\partial x_1 &= \alpha_1 - \beta w_1^* - 2\beta x_1 - (\alpha_2 - \beta w_2^*) - 2\beta x_1 \\ &= -8 - 4x_1.\end{aligned}$$

The optimal response of the owner of storage is $x_1^* = -2$ and $x_2^* = 2$ to maximize its profits.

However, as Table I shows, a solution exists in the joint mode (which is, in fact, the optimal solution) that fulfills the constraints of Problem (3) and yields a higher overall profit compared to the disjoint mode. This outcome is an example of the "prisoner's

dilemma", where two self-interested players making individual decisions will ultimately lead to a suboptimal choice for both parties [23]. It highlights the fact that cooperation may not always be in one's best interest.

Although the overall profit is higher under the joint operation mode, the value of energy storage is not necessarily higher for the RES generator. Under the price-maker setting, Π^*_{ORI} does not equal Π^*_{RES}. For instance, in Example 1, $\Pi^*_{\text{ORI}} = 3 \times (15 - 3) + 15 \times (35 - 15) = \$336$, which differs from $\Pi^*_{\text{RES}} = \$312$. Therefore, the value of energy storage for the RES owner is $\Pi^*_{\text{Joint}} - \Pi^*_{\text{ORI}} = 338 - 336 = \$2$; However, its value would be \$8 for the independent arbitraging entity. This example illustrates that there are instances where energy storage may hold greater value for an arbitrageur compared to an RES generator. However, a definitive comparison between the value of energy storage for an RES owner versus solely for an arbitrageur cannot be established. The empirical analysis presented in Section V further explores this question.

III. Stochastic Adaptive Model

The deterministic model of Section II overlooks the inherent uncertainty associated with the output of RES. As a result, it neglects the additional value that energy storage provides the RES owner by avoiding or reducing the penalties incurred when the actual production deviates from the ex-ante commitment. This section expands the deterministic model to include the sources of uncertainty and assesses their potential impact on the comparison between the ownership structures. To replicate the dynamics of actual electricity markets, we use a two-stage adaptive model, comprising a day-ahead market and a real-time market. The sequential decision-making process unfolds as follows:

- In the day-ahead market, participants employ stochastic optimization for submitting bids, i.e., $\boldsymbol{w}^{\mathbf{D}}$ and $\boldsymbol{x}^{\mathbf{D}}$.
- The subsequent real-time market, known as the settlement phase, enables participants to submit revised bids, i.e., $\boldsymbol{w}^{\mathbf{R}}$ and $\boldsymbol{x}^{\mathbf{R}}$. This adjustment is in response to actual conditions, including RES output and real-time price.

Remark: Our study adopts a two-stage model for simplicity, consistent with common approaches in the literature. While a multi-stage model (refer to [12] and [24]) more accurately reflects time-evolving uncertainty, this complexity extends beyond our paper's focused scope.

We make the following assumptions to be able to focus on the specific impacts of uncertainty:

Assumption 1: Decision-makers have access to day-ahead electricity prices (p^D_t), whereas the real-time electricity prices ($\widetilde{p}^R_t$) are inherently unpredictable in advance.

Assumption 2: All the agents are price-takers.

Remark: Section II explores the price-maker setting within a deterministic framework, revealing its effect on ownership structure differences. Given that deterministic scenarios are specific instances of broader stochastic models, similar outcomes can be inferred. Therefore, this section adopts a price-taker approach to concentrate on examining risk preferences.

Our optimization problems commence with a generic risk measure (ρ), which represents the expected value ($\mathbb{E}$) under conditions of risk neutrality, and embodies the Conditional Value at Risk (CVaR) in scenarios where risk aversion is prevalent.

A. General Two-Stage Optimization: Disjoint Mode

In this subsection, the RES owner and the separate entity make decisions independently. Decisions made for the day-ahead market are predetermined; conversely, the real-time market bids and curtailments are adjustable, acting as recourse variables in our adaptive framework. Consequently, w^R_t and w^c_t must be modeled as functions dependent on the uncertain variables at time t, specifically $\widetilde{p}^R_t$ and $\widetilde{w}_t$. Problem (4) defines the disjoint operation of the RES.

$$\max_{\boldsymbol{w}^{\mathbf{D}}} \ \boldsymbol{p}^{\mathbf{D}\dagger}\boldsymbol{w}^D + \boldsymbol{\rho}\left[\max_{\boldsymbol{w}^{\mathbf{R}}\in\Omega^W(\boldsymbol{w}^{\mathbf{D}},\widetilde{\mathbf{p}}^{\mathbf{R}\dagger},\widetilde{\mathbf{w}})} \widetilde{\mathbf{p}}^{\mathbf{R}\dagger}\boldsymbol{w}^{\mathbf{R}}\right] \tag{4a}$$

$$s.t. \quad w^D_t \geq 0, \ \forall t. \tag{4b}$$

The feasible region of w^R_t is defined in (5).

$$\Omega^W_t(w^D_t, \widetilde{p}^R_t, \widetilde{w}_t) := \{\ w^D_t + w^R_t = \widetilde{w}_t - w^c_t, \ \forall t, \tag{5a}$$

$$0 \leq w^c_t \leq \widetilde{w}_t, \ \forall t\ \}. \tag{5b}$$

Constraint (4b) restricts the RES owner to be a "sell-only" agent on the day-ahead market. Constraint (5a) ensures that the total amount of electricity committed by the RES owner in the day-ahead market, along with any adjustments made through real-time bids, matches its actual generation. For example, if $w^D_t > \widetilde{w}_t$, the RES owner procures the deficit electricity from the market to cover the shortfall; Conversely, RES can sell the surplus electricity for additional revenue. Constraint (5b) defines the range of curtailment amount.

In analogy to the RES model, x^R_t, d^F_t, c^F_t, and S^F_t in the storage model also adapt to the realization of $\widetilde{p}^R_t$. Problem (6) describes the disjoint operation of the storage.

$$\max_{\boldsymbol{x}^{\mathbf{D}}} \ \boldsymbol{p}^{\boldsymbol{D}\dagger}\boldsymbol{x}^{\boldsymbol{D}} + \boldsymbol{\rho}\left[\max_{\boldsymbol{x}^{\mathbf{R}}\in\Omega^X(\boldsymbol{x}^{\mathbf{D}},\widetilde{\mathbf{p}}^{\mathbf{R}})} \widetilde{\mathbf{p}}^{\mathbf{R}\dagger}\boldsymbol{x}^{\mathbf{R}}\right] \tag{6a}$$

$$s.t. \quad x^D_t = d^D_t - c^D_t, \ \forall t, \tag{6b}$$

$$S^D_{t+1} = S^D_t - \frac{1}{\eta_d} d^D_t + \eta_c c^D_t, \ \forall t, \tag{6c}$$

$$0 \leq d^D_t \leq L, \quad 0 \leq c^D_t \leq L, \ \forall t, \tag{6d}$$

$$0 \leq S^D_t \leq \bar{S}, \ \forall t, \quad S^D_0 = S^D_T = \frac{1}{2}\bar{S}. \tag{6e}$$

The feasible region of x^R_t is defined in (7).

$$\Omega^X_t(x^D_t, \widetilde{p}^R_t)$$

$$:= \left\{ x^D_t + x^R_t = d^F_t - c^F_t, \ \forall t, \right. \tag{7a}$$

$$S^F_{t+1} = S^F_t - \frac{1}{\eta_d} d^F_t + \eta_c c^F_t, \ \forall t, \tag{7b}$$

$$0 \leq d^F_t \leq L, \quad 0 \leq c^F_t \leq L, \ \forall t, \tag{7c}$$

$$0 \le S_t^F \le \bar{S},\ \forall t, \quad S_0^F = S_T^F = \frac{1}{2}\bar{S} \Big\}. \tag{7d}$$

Constraints (6b) to (6e) force the day-ahead bids to respect the operational limitations. Constraint (7a) forces the actual discharge or charge from the storage to reflect the cumulative effect of the bids at both the day-ahead and real-time stages. Constraints (7b) to (7d) impose restrictions on the actual operation of the energy storage.

B. General Two-Stage Optimization: Joint Mode

When the storage is owned by the RES owner, it is often integrated with the RES generator to jointly manage the mismatch between the day-ahead bids and the actual outputs of the RES generator. To emphasize this collaboration at the real-time stage, we assume that the RES owner and the energy storage system operate separately at the day-ahead phase. Problem (8) formulates the joint operation.

$$\max_{\boldsymbol{w}^{\mathbf{D}},\boldsymbol{x}^{\mathbf{D}}} \ \boldsymbol{p}^{\mathbf{D}\dagger}\left(\boldsymbol{w}^{\mathbf{D}} + \mathbf{x}^{\mathbf{D}}\right) \tag{8a}$$

$$+\boldsymbol{\rho}\left[\max_{(\boldsymbol{w}^{\mathbf{R}},\boldsymbol{x}^{\mathbf{R}})\in\Omega^J(\boldsymbol{w}^{\mathbf{D}},\boldsymbol{x}^{\mathbf{D}},\widetilde{\mathbf{p}}^{\mathbf{R}\dagger},\widetilde{\mathbf{w}})} \widetilde{\mathbf{p}}^{\mathbf{R}\dagger}\left(\boldsymbol{w}^{\mathbf{R}} + \mathbf{x}^{\mathbf{R}}\right)\right] \tag{8b}$$

$$s.t. \quad \text{Constraint (4b)}, \tag{8c}$$

$$\text{Constraints (6b)} - \text{(6e)}. \tag{8d}$$

The feasible region of w_t^R and x_t^R is defined in (9).

$$\Omega_t^J(w_t^D, x_t^D, \widetilde{p}_t^R, \widetilde{w}_t)$$

$$:= \{\, w_t^D + x_t^D + w_t^R + x_t^R = \widetilde{w}_t - w_t^c + d_t - c_t,\ \forall t, \tag{9a}$$

$$\text{Constraint (5b)}, \tag{9b}$$

$$\text{Constraints (7b)} - \text{(7d)}\ \}. \tag{9c}$$

As Constraint (9a) shows, the RES and the storage collaboratively determine the amount of energy to be purchased or sold in the real-time markets to address any imbalance. In the event of a deficit, rather than solely relying on purchasing electricity from the market, the energy storage system has the ability to discharge stored energy, avoiding the potentially high real-time electricity purchase price. Conversely, the storage system can charge and sell the stored energy in the future when prices are anticipated to be higher. This constraint can also be mathematically regarded as a composition of Constraints (5a) and (7a). Constraints (8c) and (8d) characterize the day-ahead stage and Constraint (9c) represents the actual operational behavior of the energy storage system.

C. Equivalence in Risk-Neutral Model

We first show the risk-neutral scenario, where $\rho[\cdot] := \mathbb{E}[\cdot]$, and have the following proposition.

Proposition 3: When agents are risk-neutral, the optimal solutions of the two disjoint operation problems i.e., (4) and (6), are also optimal solutions to the joint operation problem i.e., (8).

Proof Sketch: First, we can derive the scenario representation (extended formulation) for each two-stage risk-neutral optimization problem, where each scenario corresponds to different real-time recourse variables, i.e., $\boldsymbol{x}_i^R$ and $\boldsymbol{w}_i^R$ for scenario i. Second, for each scenario, Constraints (5a) and (7a) can be regarded as a way of decomposing Constraint (9a) to decouple the decision variables. The remaining steps of the proof follow a similar structure to that of Proposition 1. Appendix C provides the details of the proof.

Given Assumption 2 i.e., $\boldsymbol{p}^R$ is exogenous, Π^*_{ORI} is equal to Π^*_{RES}. As a result, Proposition 3 shows that $\Pi^*_{\text{Joint}} - \Pi^*_{\text{ORI}} = \Pi^*_{\text{Joint}} - \Pi^*_{\text{RES}} = \Pi^*_{\text{Storage}}$. In other words, the value of the energy storage system for an RES owner is equivalent to that of an independent energy arbitrageur, assuming all agents are price-takers and risk-neutral.

D. Distinction in Risk-Averse Model

CVaR is frequently preferred as the risk measure for representing risk-averse scenarios as it provides a more comprehensive view of the expected profits in less favorable conditions, particularly focusing on the tail-end of the distribution. Notably, CVaR of the profit Π pertaining to the $(1-\alpha)$-quantile is defined as the conditional expectation of Π given that Π does not exceed the value at risk (VaR) of Π, as shown in (10):

$$\rho[\Pi] := \text{CVaR}_{1-\alpha}[\Pi] = \mathbb{E}[\Pi|\Pi \le \text{VaR}_{1-\alpha}[\Pi]],$$

$$\text{VaR}[\Pi] = \max\{v|F_\Pi(v) \le 1-\alpha\}. \tag{10}$$

It's important to note that risk-averse levels may vary between energy storage and RES owners, meaning α_w and α_x can differ. Proposition 4 applies to the risk-averse model.

Proposition 4: When agents are risk-averse, the optimal dispatch decisions are derived from the two disjoint operation problems and may not be optimal for the joint problem.

Illustrative Example 2 demonstrates Proposition 4.

Example 2: To explore how joint and disjoint operations differ under the CVaR framework, we focus on a scenario where risk-averse stochastic programming converges to adaptive robust optimization. Specifically, as α approaches to 1, $\lim_{\alpha\to 1}\text{CVaR}_{1-\alpha}[\Pi] = \inf_{\theta\in\Theta}[\Pi]$, in line with [25]. In this adaptive robust optimization context, the objective is to maximize profits while considering the most unfavorable cases of RES power output and real-time pricing. Therefore, the risk measure $\rho[\cdot]$ can be characterized by $\min_{\widetilde{\mathbf{p}}^{\mathbf{R}}\in\boldsymbol{\mathcal{P}},\widetilde{\boldsymbol{w}}_t\in\boldsymbol{\mathcal{W}}_t}[\cdot]$. In this example, $T = 2$. The day-ahead electricity prices are $p_1^D = 20\$$ /MWh, $p_2^D = 25\$$/MWh. The uncertainty set of the actual RES output is $\widetilde{w}_1 \in [15, 20]$, $\widetilde{w}_2 \in [20, 25]$. The uncertainty set of the real-time price is $p_1^r \in [25, 40]$, $p_2^r \in [35, 40]$. The example assumes no correlation between actual RES output and real-time prices. The parameters of the storage are $\eta_c = \eta_d = 1$, $L = 5\,\text{MWh}$, and $\bar{S} = 10\,\text{MWh}$.

We first calculate the optimal strategy of each agent for disjoint operation. The optimal strategy for the individual RES owner is always $w_t^D = 0$ and $w_t^R = \widetilde{w}_t$ since the real-time price is always higher than the day-ahead price in this example. As for the storage owner, the worst scenario for real-time prices is

TABLE II
COMPARISONS BETWEEN TWO FEASIBLE SOLUTIONS IN THE JOINT OPERATION MODE IN EXAMPLE 2

	Stage	Day-ahead w^D	Day-ahead x^D	Real-time $w^{R*}+x^{R*}$	Profit
Opt 1	1	0	-5	$\widetilde{w}_1$	$25+25\widetilde{w}_1+35\widetilde{w}_2$
	2	0	5	$\widetilde{w}_2$	
Opt 2	1	0	0	$\widetilde{w}_1-5$	$50+25\widetilde{w}_1+35\widetilde{w}_2$
	2	0	0	$\widetilde{w}_2+5$	

$p_1^{R*}=p_2^{R*}$, and its optimal strategy at the day-ahead stage is $x_1^D=-5$ and $x_2^D=5$. Refer to Appendix D for the details.

For joint operation, the worst scenario for real-time prices is $p_1^{R*}=25, p_2^{R*}=35$, and the worst scenario for RES output is $\widetilde{w}_1^*=15, \widetilde{w}_2^*=20$. (Again, refer to Appendix D for the details.) Under this scenario, it is optimal to charge the storage during the first period and discharge it during the second period, as the prices during the second period are higher, i.e., $x_1^{R*}+w_1^{R*}=\widetilde{w}_1+L-x_1^D-w_1^D$, $x_2^{R*}+w_2^{R*}=\widetilde{w}_2-L-x_2^D-w_2^D$. Table II compares two feasible solutions for the RES for joint operation. "Opt 1" represents the approach where the day-ahead decisions align with the optimal solutions in the disjoint operation mode. However, if the combined agent chooses not to join the day-ahead market in the joint operation, which is "Opt 2" in Table II, the profit increases by \$25 compared to "Opt 1". Hence, the optimal solution in the disjoint operation mode does not align with that in the joint operation mode.

Proposition 4 highlights that Π^*_{Joint} can differ from $\Pi^*_{\text{RES}}+\Pi^*_{\text{Storage}}$ when agents are risk averse. Hence, energy storage can yield varying values for the two types of owners. In Example 2, we observe that $\Pi^*_{\text{Joint}}\geq 50+25\times 15+35\times 20=1125$, $\Pi^*_{\text{ORI}}=\Pi^*_{\text{RES}}=\geq 25\times 15+35\times 20=1075$, and $\Pi^*_{\text{Storage}}=20\times(-5)+25\times 5=25$. Consequently, the value for the RES owner exceeds \$50, while the value for an independent arbitrageur is less at \$25.

IV. DISCUSSION OF ADDITIONAL FACTORS

In this section, we examine special circumstances where the value of storage differs between the two ownership structures, even when both agents are price-takers and risk-neutral.

A. Differential Pricing

In Sections II and III, we assumed that electricity prices are uniform for all agents. However, there are situations where this assumption is not valid and where price differences have an effect on how ownership affects the value of storage.

1) Two-Price Settlement: Some real-time balancing markets have implemented a two-price settlement rule [26] where the price for purchasing power (p_t^b) can be considerably higher than the price at which electricity can be sold back to the grid (p_t^s), i.e., $p_t^b>p_t^s$.

Proposition 5: Under the assumption of risk neutrality and a two-price settlement rule, the value of energy storage is higher for the RES owner compared to an independent arbitrageur.

While the Appendix E provides detailed proof of this proposition, it can be intuitively explained as follows. If the RES owner over-commits at the day-ahead stage, storage can mitigate the resulting mismatch and avoid the higher cost of buying energy from the market. Similarly, if the RES has excess energy to sell, storage can store it to avoid selling at a lower price in real time.

2) Congestion: In Sections II and III, we assumed that energy storage and RES are co-located. As pointed out in [27], placing them separately at their most advantageous locations could result in improved price profiles and better utilization of interconnection capacity, leading to better profits from the disjoint operation.

B. Market Access

Two potential market barriers challenge some assumptions made in Section II and Section III.

1) "sell-Only" Restriction: In Proposition 1 of the deterministic case, we treated joint operation as a "two-way trading" scenario. However, there can be "sell-only" restrictions, which limit the RES owner to solely shift the RES output between periods for selling purposes, thereby prohibiting the RES from purchasing energy from the market and engaging in arbitrage activities [5]. This imposes a new constraint (11) in Problem (3).

$$x_t+w_t\geq 0,\ \forall t. \tag{11}$$

Since $\Pi_{\text{Joint}_{\text{Mono}}}\leq\Pi_{\text{Joint}}$ due to the reduced feasible space, $\Pi_{\text{Joint}_{\text{Mono}}}-\Pi_{\text{ORI}}\leq\Pi_{\text{Storage}}$. This implies that if there are market barriers to the use of energy storage by the RES owner, the value of energy storage is greater for an arbitrageur than for an RES owner, assuming all agents are price-takers.

2) Ancillary Service (AS) Market: We posit that energy storage can generate additional profit from the AS products, specifically through up-regulation and down-regulation capacity. In the day-ahead market, bids for regulation services are usually cleared for each energy dispatch period. Resources committed to regulation service must be available during specific intervals to adjust their output for grid stability. This introduces a new constraint (12) to replace Constraint (6e) in the day-ahead operation of storage systems, i.e., Problem (6).

$$\begin{aligned}&0\leq r_t^U\leq L,\quad 0\leq r_t^L\leq L,\ \forall t,\\&0\leq r_t^U+d_t^D\leq L,\quad 0\leq r_t^L+c_t^D\leq L,\ \forall t,\\&\frac{1}{\eta_d}r_t^U\leq S_t^D\leq\bar{S}-\eta_c r_t^L,\ \forall t,\ S_0^D=S_T^D=\frac{1}{2}\bar{S}.\end{aligned} \tag{12}$$

In the real-time market, resources might be called upon at higher frequencies to respond to the immediate actual need for regulation service, rather than a preset dispatch period. Hence, Constraints (7a) through (7c) are replaced by Constraint (13) to represent the multi-timeframe optimization effectively.

$$x_t^D+x_t^R+\widetilde{\tau}_{t,k}^U r_t^U-\widetilde{\tau}_{t,k}^L r_t^L=d_{t,k}^F-c_{t,k}^F,\ \forall t,\forall k, \tag{13a}$$

$$S_{t+1}^F=S_t^F-\frac{1}{\eta_d K}\sum_{k=1}^K d_{t,k}^F+\frac{\eta_c}{K}\sum_{k=1}^K c_{t,k}^F,\ \forall t, \tag{13b}$$

TABLE III
COMPARATIVE ANALYSIS OF OWNERSHIP TYPES ACROSS CONDITIONS

Condition	Two-Price Settlement	Congestion	RES: "Sell-Only"	Ancillary Service
RES Owner	✔	✗	✗	✔
Arbitrageur	✗	✔	✔	✔

$$0 \le d^F_{t,k} \le L, \quad 0 \le c^F_{t,k} \le L, \ \forall t, \forall k. \tag{13c}$$

On the other hand, the studies in [21] and [12] show that joint operations can also earn additional profits by dispatching energy storage for regulation service. Detailed formulations are in Appendix F. Mirroring the proof for Proposition 3, when both agents are price-takers, the value of storage remains the same for the RES owner and the arbitrageur.

In summary, Table III specifically contrasts the two types of ownership and delineates which is more advantageous in each condition discussed within this section.

V. CASE STUDY

This case study primarily aims to conduct a numerical comparison of scenarios that yield varying energy storage values for both the RES owner and the independent arbitrageur. Specifically, it focuses on the scenarios outlined in Section II-D, Section III-D, and IV. We aim to quantitatively estimate the magnitude of the gap between these values and study the impact of various factors. The deterministic optimization problems are solved utilizing the Gurobi solver while the stochastic optimization problems are addressed with the CVX [28] toolbox.

A. Price-Maker Scenario

First, we assume that agents have perfect foresight on prices and RES output to evaluate the model introduced in Section II-D. We use synthetic data extracted from open-source datasets and reports of the Electric Reliability Council of Texas (ERCOT). Fig. 3(a) presents the merit order curve of traditional generators derived from [29], which ranks bids in ascending order of marginal price. We fit a three-segment piece-wise linear function to this curve. Each segment has its own coefficient and intercept. Fig. 3(b) depicts the net load curve, derived from data in [30]. This curve represents the difference between the grid's total electricity demand and the combined electricity generation from all renewable resources at any given moment. The solid lines show the average values and the padding represents the error band, with different colors for each season. Fig. 3(c) and (d) depict the typical daily generation profile of RES, represented by the ratio of actual output to the installed capacity [31]. The lines in the graph represent average values, and the bars indicate the range from minimum to maximum values. Distinctions between solar and wind generation across the four seasons are emphasized through varying colors.

The residual demand curve of each hour is based on the merit order curve and the net load profile curve. Specifically, if the net load at time t is L_t, the market-clearing price at that time is determined by the intersection of the merit order curve with the vertical line that intersects the x-axis at arbitrageur value of $L_t - (w_t + x_t)$. During the summer, electricity prices are sensitive to the selling bids from storage and RES. For instance, the residual demand curve exhibits a steep slope, reaching as high as -2.28 USD/(MWh·GW) during periods of heavy load. In contrast, the electricity price shows relatively less sensitivity in winter, as the slope of the residual demand curve tends to remain mostly flat, typically around -0.12 USD/(MWh·GW). We analyze four scenarios based on seasonal variations (summer and winter) and the types of RES generation (solar and wind). For simplicity, we assume full round-trip efficiency for energy storage. When the energy storage and the RES generator capacity are both 2 GW, Fig. 4 compares the average value generated by storage during a day for the RES owner and the arbitrageur under these four scenarios, respectively.

Specifically, in the "Mono" scenario, a RES owner is restricted to a "sell-only" model, prohibited from charging from the grid. Due to greater price volatility, the value of storage tends to be higher during the summer compared to winter, enabling storage to be more effective. Furthermore, Fig. 5 visualizes the bidding decisions and clearing prices for each scenario, offering detailed insights into the findings presented in Fig. 4. We present the bidding decisions in intervals of three hours as a representative demonstration. In particular, the labels "RES True" indicate the

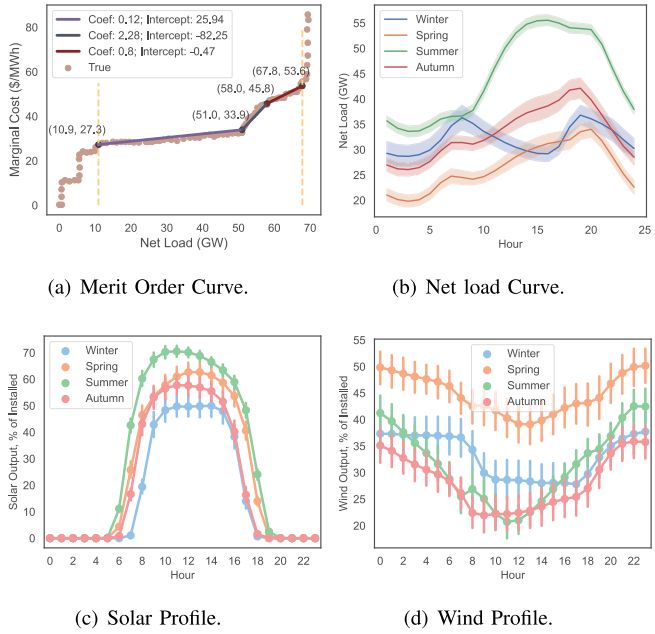

(a) Merit Order Curve. (b) Net load Curve.

(c) Solar Profile. (d) Wind Profile.

Fig. 3. Information and parameters related to ERCOT.

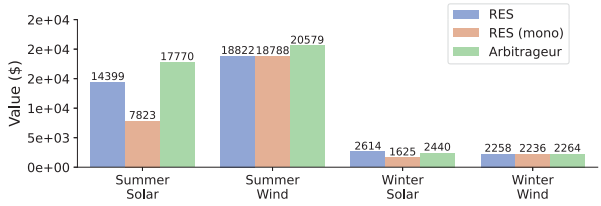

Fig. 4. Comparison of the value for the RES owner and the arbitrageur.

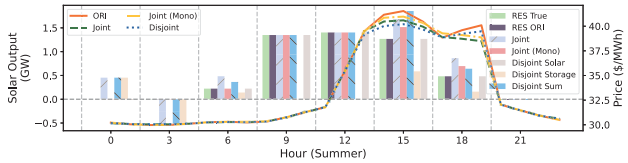

(a) Solar Panel during Summer.

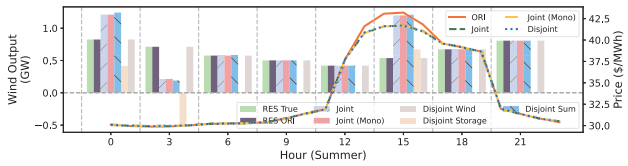

(b) Wind Turbine during Summer.

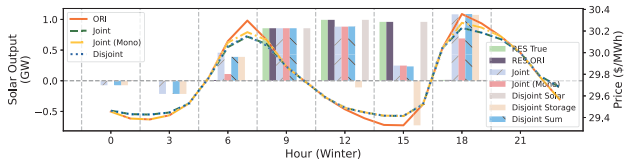

(c) Solar Panel during Winter.

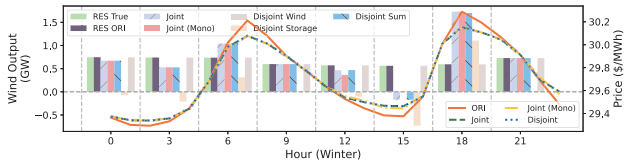

(d) Wind Turbine during Winter.

Fig. 5. Bidding decisions and clearing prices throughout a typical day.

actual output of the RES generator, while "RES ORI" represents the bidding decision of RES without additional energy storage. As is shown in Fig. 5(a), during summer, storage holds greater value for an arbitrageur compared to an RES owner, regardless of the RES type. The reason is two-fold. First, although the RES owner can sell more energy during high-price hours, the market-clearing price is significantly lower for the joint operation scenario compared to the stand-alone RES generator scenario, for example, at $18:00$, which largely weakens the value of energy storage for an RES owner. On the other hand, energy storage demonstrates greater flexibility when operated independently, enabling it to leverage the volatile price dynamics to maximize its own value. For instance, at $6:00$ when the electricity price is relatively low, the storage discharges a lesser amount compared to the joint operation. In contrast, at $15:00$ when the electricity price reaches its peak, the storage charges more extensively compared to the joint operation. This principle also holds in the context of a wind-type RES during summer, though the benefits of flexibility are less pronounced, as is shown in Fig. 5(b). Conversely, as depicted in Fig. 5(c), during winter, a solar RES owner with grid charging access finds the storage to be of greater value compared to the arbitrageur. This difference is primarily due to the distinctive profiles of solar RES output and electricity prices. At $15:00$, when the electricity price is low and solar output is high, energy storage enables the solar RES owner to store excess energy and sell it during periods of higher

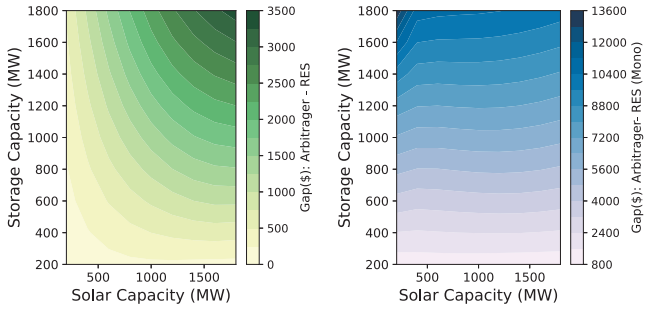

(a) Arbitrageur and RES. (b) Arbitrageur and RES (Mono).

Fig. 6. Impact of RES and storage capacity on the gap in the value of storage (summer solar).

prices, such as at $18:00$. This strategy proves more valuable than profiting solely from arbitrage. Meanwhile, as illustrated in Fig. 5(d), the generation profiles of joint and separate operations involving a wind-type RES during winter show a high degree of similarity, leading to almost equivalent values for both the RES owner and the arbitrageur.

Furthermore, despite the season or type of RES, it's clear that imposing "sell-only restrictions" on RES owners significantly reduces the value of energy storage for them, in contrast to arbitrageurs. This phenomenon is particularly prominent for solar RES owners, as they primarily profit from arbitrage activities supported by grid charging during the period from $20:00$ to $7:00$ (next day). Fig. 6 shows the influence of the capacity of storage and RES on the gaps between the values of storage for RES owner and arbitrage, using solar RES during the summer as an illustration. In the case of solar RES with grid charging access, the value gap increases monotonically with both solar and storage capacity. However, when grid charging is restricted, the gap is primarily influenced by the storage capacity.

B. Comparison Between Risk-Neutral and Risk-Averse Model

Similar to Section III, this case study is based on the premise that storage and RES are price-takers. In both the risk-neutral and risk-averse models, both the storage and the RES generator have a 1 GW capacity, with a 20% per hour ramp rate for storage.

The market price information is constructed from historical prices of ERCOT day-ahead and real-time markets [32]. We arbitrarily choose the trading hub "HB_South" for siting storage and RES, and select the day-ahead price data for "August 01, 2022" as the basis for our optimization input. As the real-time price is typically considered the adjustment amount received by participants for deviations from the day-ahead commitments, the relative difference between the day-ahead price and the real-time price of every hour is a random variable, i.e., $(p_t^r - p_t^D)/p_t^D$. We assume that this variable maintains a consistent distribution across all trading hubs and throughout the entire year. Therefore, the samples for real-time prices are constructed based on this relative difference using the day-ahead and the corresponding real-time price in 2022. We then use 706 samples as training data to formulate day-ahead decisions (referred to as in-sample

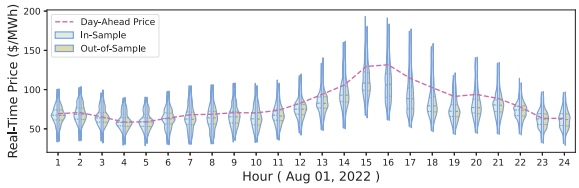

(a) Real-time Price.

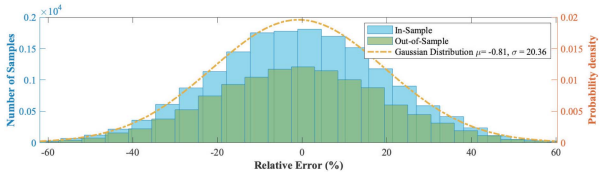

(b) Deviation between Actual RES Output's and Forecast.

Fig. 7. Characterization of in-samples and out-of-samples data.

data) and reserve an additional 472 samples for subsequent out-of-sample analysis. Fig. 7(a) illustrates the trajectory of the day-ahead prices and the distribution of in-sample and out-of-sample data points of the real-time prices for each hour. Additionally, the forecasted RES output data is extracted from ERCOT's average wind turbine profile for the summer of 2022 [31]. Actual RES output samples are generated by sampling from the distribution of relative forecast error, which is estimated in [33] to follow a Gaussian distribution. Fig. 7(b) provides the distribution parameters and presents the in-sample and out-of-sample data of the deviation between the actual RES output and the forecast. We assume independence between the relative differences in day-ahead versus real-time prices and the relative forecast errors.

Drawing from the in-sample data, we first address the two-stage adaptive optimization problems for both risk-neutral and risk-averse models, encompassing joint and disjoint operations. Specifically, we consider Problem (4), Problem (6) and Problem(8) with risk measures set as $\rho := \mathbb{E}$ and $\rho := \text{CVaR}_{1-\alpha}$, respectively. In the risk-averse model, we explore two scenarios: (i) where the arbitrageur and the RES owner share the same level of risk aversion, denoted as $\alpha_w = \alpha_x = 0.95$; (ii) where the arbitrageur exhibits a lower level of risk aversion compared to the RES owner, with $\alpha_w = 0.95$ and $\alpha_x = 0.7$. Each model yields its respective optimal day-ahead decision variables, i.e., w_*^D and x_*^D. With these day-ahead decisions as inputs, we proceed to solve the deterministic version of real-time optimization problems for each out-of-sample data, from which we compute the mean (Avg) and standard deviation (Std) of the optimal profits. The deterministic formulation is provided in Appendix G and the detailed process of the out-of-sample analysis is shown in [34]. Table IV presents the in-sample and out-of-sample results. Notably, in the risk-neutral model, both the joint and disjoint operation problems yield the same optimal values for both in-sample and out-of-sample data, providing empirical support for Proposition 3. As a result, the values for the arbitrageur and RES are identical. Conversely, in the risk-averse model, the optimal values for the joint and disjoint operation problems can differ, thereby confirming Proposition 4. In this case study, it is evident that, in both

TABLE IV
OPTIMIZATION RESULTS FOR IN-SAMPLE AND OUT-OF-SAMPLE DATA

Method	Type	Risk-Neutral ($\times 10^3$\$)	Risk-Averse ($\times 10^3$\$) (0.95, 0.95)	Risk-Averse ($\times 10^3$\$) (0.95, 0.7)
In -Sample	Joint	**945.98**	**778.45**	**778.45**
	Disjoint Storage	71.19	59.83	62.58
	Disjoint RES	874.79	709.04	709.04
	Disjoint Sum	**945.98**	**768.87**	**771.62**
	Value for RES	***71.19***	***69.41***	***69.41***
	Value for Arbitrageur	***71.19***	***59.83***	***62.58***
Out-of -Sample	Joint: Avg	**946.59**	**883.65**	**883.65**
	Joint: Std	94.29	51.76	51.76
	Disjoint Storage: Avg	71.40	69.48	69.79
	Disjoint Storage: Std	9.22	7.47	7.43
	Disjoint RES: Avg	875.18	800.36	800.36
	Disjoint RES: Std	92.85	43.98	43.98
	Disjoint Sum: Avg	**946.59**	**869.84**	**870.16**
	Disjoint Sum: Std	94.29	46.21	46.20
	Value for RES: Avg	***71.40***	***83.28***	***83.28***
	Value for RES: Std	9.22	13.44	13.44
	Value for Arbitrageur: Avg	***71.40***	***69.48***	***69.79***
	Value for Arbitrageur: Std	9.22	7.47	7.43

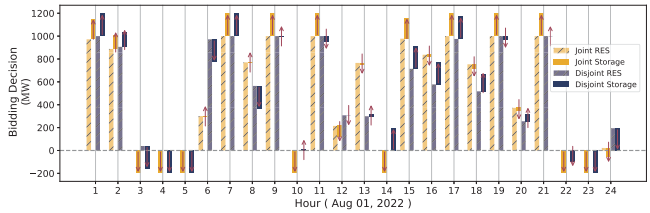

Fig. 8. Comparison of risk-averse day-ahead decisions ($\alpha_w = \alpha_x = 0.95$).

risk-averse scenarios, the value for the RES exceeds that of the arbitrageur. Furthermore, the out-of-sample results indicate that adopting a risk-averse approach leads to reduced optimal profits compared to the risk-neutral model. However, the standard deviation is also smaller, suggesting a more stable and less volatile outcome.

Specifically, we compare day-ahead decisions for the joint and disjoint modes within the context of the risk-averse model in Fig. 8, where $\alpha_w = \alpha_x = 0.95$. The storage decision is visually depicted as a bar positioned atop the RES decision value, which enables a clear presentation of the cumulative effect for better comparison. An upward arrow signifies storage discharging and a downward arrow indicates storage charging. By integrating information from both Figs. 7 and 8, it becomes evident that during hours when real-time prices display greater uncertainty, particularly between 14:00 and 18:00, the decisions for joint and disjoint modes can markedly diverge. In some cases, the storage decisions may even be contrary to one another. This divergence can be intuitively attributed to varying interpretations of what constitutes a "risky" scenario for different agents involved in the decision-making process.

C. Impact of Additional Factors

In this subsection, we assume both agents take a risk-neutral perspective, in order to exclusively focus on the influence of additional factors discussed in Section IV. The datasets remain consistent with those in Section V-B.

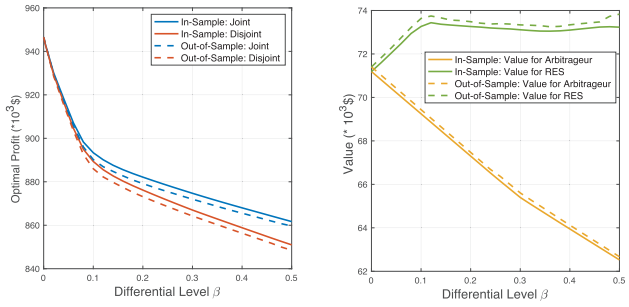

(a) Optimal Profits. (b) Value for Arbitrageur and RES.

Fig. 9. Impact of differential level for the two-price real-time markets.

1) Two-Price Real-Time Market: First, we analyze the two-price settlement scheme within the real-time market. We introduce an index referred to as the 'differential level', symbolized by β, to quantify the disparity between the selling and buying prices. Accordingly, for each sample denoted by i, we establish the following relationships: the selling price at time t, $p^s_{i,t}$, is calculated as $p^r_{i,t}$ multiplied by $(1-\beta)$ and the buying price at time t, $p^b_{i,t}$, is determined as $p^r_{i,t}$ multiplied by $(1+\beta)$. The optimal profits for joint and disjoint operations, as illustrated in Fig. 9(a), validate Proposition 5 by confirming that, when $\beta > 0$, the optimal profits for joint operation always exceeds that of disjoint operation. As β escalates, the buying price rises while the selling price declines in the real-time markets, leading to a decrease in the optimal results for both operation problems. The disparity between the two optimal results widens as β increases, which can be attributed to the joint operation's enhanced coordination of storage and RES management to effectively reduce the expensive deviations from day-ahead commitments. Additionally, Fig. 9(b) demonstrates that the value of storage for RES remains superior to that of arbitrageur when $\beta > 0$. The value for the arbitrageur diminishes as the differential level rises, whereas the value for RES experiences a slight initial increase before stabilizing. In light of the comparative advantages, it is more advantageous for storage assets to be held by RES in a two-price real-time market context.

2) Congestion: We investigate an additional scenario where the storage and RES are owned and operated independently and situated at separate locations. This contrasts with a joint operation model where both entities are co-located, potentially leading to congestion. Since congestion is typically manifested through locational marginal prices (LMPs), our analysis focuses on understanding how variations in LMPs across different locations influence profitability. Utilizing historical day-ahead LMP data from various ERCOT network trading hubs [32], we generate real-time price samples for each hub using the same methodology outlined in Section V-B. When the RES generator and energy storage are co-located at the trading hub "HB_South", the value of the energy storage is identical for both the RES generator and the arbitrageur, amounting to 7.119×10^4 USD. However, Table V shows the potential value of energy storage for an arbitrageur located at different sites based on the in-sample dataset. It is evident that if the energy storage system is deployed in load zone "LZ_AEN" and dedicated primarily to arbitrage activities,

TABLE V
VALUE FOR ARBITRAGEUR LOCATED ON A SEPARATE SITE

Location	Value for Arbitrageur ($\times 10^3$\$)	Location	Value for Arbitrageur ($\times 10^3$\$)
HB_SOUTH	71.19	LZ_HOUSTON	81.22
HB_NORTH	89.86	LZ_LCRA	109.03
HB_PAN	92.62	LZ_NORTH	90.22
HB_HOUSTON	81.17	LZ_RAYBN	91.01
HB_WEST	88.91	LZ_SOUTH	69.65
LZ_AEN	109.89	LZ_WEST	102.09

TABLE VI
PROFITS INFORMATION FOR RES OWNER AND ARBITRAGEUR INCORPORATING AS SERVICE GIVEN DIFFERENT q_u AND q_l

(q_u, q_l)	$(0.2, 0.2)$	$(0.2, 0.1)$	$(0.1, 0.2)$
Joint Profit ($\times 10^3$\$)	1094.13	1076.33	1107.13
Energy (%)	89.69	89.56	89.47
Regulation Up (%)	7.28	7.40	7.53
Regulation Down (%)	3.04	3.04	3.00
Relative Increase (%)	15.66	13.78	17.03
Value for RES ($\times 10^3$\$)	**219.34**	**201.53**	**232.33**
Arbitrageur Profit ($\times 10^3$\$)	219.34	201.53	232.33
Energy (%)	48.55	44.26	49.80
Regulation Up (%)	36.30	39.51	35.90
Regulation Down (%)	15.14	16.23	14.30
Relative Increase (%)	208.09	183.09	226.35
Value for Arbitrageur ($\times 10^3$\$)	**219.34**	**201.53**	**232.33**

there is a considerable advantage compared to coupling it with the RES.

3) AS Market: The day-ahead clearing prices for up-regulation and down-regulation are derived from the ERCOT capacity clearing price dataset on August 01, 2022 [32]. Real-time AS product calls for up and down regulation are set at 5-minute intervals, implying $K = 12$. The actual real-time deployment proportions for both up and down regulation capacities at each time interval are modeled using a mixture distribution. This distribution combines a binomial and a uniform distribution, represented by: $\mathbb{P}(\widetilde{\tau}^U_{t,k} = 0) = 1 - q^U, \mathbb{P}(\widetilde{\tau}^U_{t,k} = x) = q^U \times \mathbf{Uniform}(\mathbf{0}, \mathbf{1}),\ \ 0 < x \leq 1$ and $\mathbb{P}(\widetilde{\tau}^L_{t,k} = 0) = 1 - q^L, \mathbb{P}(\widetilde{\tau}^L_{t,k} = x) = q^L \times \mathbf{Uniform}(\mathbf{0}, \mathbf{1}),\ 0 < x \leq 1$. Table VI illustrates the profits derived from participation in both the energy market and the AS market based on in-sample data. The term "Relative increase" signifies the enhancement in profits compared to scenarios where participation is limited exclusively to the energy market, excluding AS markets. The profit baselines are stated in the risk-neutral model in Section V-B, which are 9.46×10^5 USD for joint operation and 7.12×10^5 USD for arbitrageur. Notably, the data reveals a substantial profit increase for storage arbitrageurs through regulation services, with almost half of their profits originating from ancillary services. The variation in results due to differing values of q_U and q_L can be attributed to their influence on operational dynamics. Specifically, a higher q_U correlates with an increased probability of more discharging activities during real-time operations, potentially diminishing the agents' opportunities for energy sales. Conversely, a higher q_L suggests more opportunities for charging the storage

TABLE VII
OPTIMIZATION RESULTS FOR STOCHASTIC PRICE-MAKER SETTING

	Profit: Avg ($\times 10^3$\$)				Value ($\times 10^3$\$)	
	Π^*_{Joint}	Π^*_{ORI}	Π^*_{RES}	Π^*_{Storage}	RES	Arbitrageur
In-Sample	937.55	867.51	867.27	70.27	70.04	70.27
Out-of-Sample	938.26	867.93	867.70	70.48	70.33	70.48

system, which is advantageous for enhancing profits from future real-time sales. Furthermore, the equal profit values for both the RES owner and the arbitrageur affirm the conclusions drawn in Section IV-B.

D. Stochastic Price-Maker Setting

In this subsection, we analyze under the assumption that both the RES owner and the arbitrageur act as price-takers in the day-ahead market, while behaving as price-makers in the real-time market. We select the slope of the residual demand curve to be -0.8 USD/(MWh·GW), in line with the third segment depicted in Fig. 3(a). This choice is informed by the typically higher marginal costs of generation in real-time markets. Consequently, the real-time market price per unit of electricity at time t for sample i is defined as $p^R_{t,i} - 8 \times 10^{-4} \times (w^R_{t,i} + x^R_{t,i})$. The in-sample and out-of-sample data explicitly inherit from the risk-neutral model in Section V-B. The optimization results are shown in Table VII, which support our conclusion that the value of storage for the RES owner and storage may vary in scenarios where they act as price-makers. Moreover, the results highlight a slightly greater importance of storage for arbitrageurs, especially in summer, as aligned with findings in Section V-A.

VI. CONCLUSION

This paper provides a systematic comparison of the energy storage's economic value for two different types of owners: the operator of renewable energy resources and a stand-alone arbitrageur. The study reveals that when both types of owners are risk-neutral and price-takers, the two ownership structures yield equivalent overall profits, which implies that energy storage has an identical value under both forms of ownership. However, when owners act as market makers or show risk aversion, the overall profits can differ between the two forms of ownership, resulting in varying values of energy storage. Special circumstances such as differential pricing and market barriers can further impact the value of energy storage for the two types of owners. A case study based on data from ERCOT provides guidelines to determine the optimal ownership structure of energy storage based on factors such as seasonality, types of renewable energy sources, and the siting of energy storage.

Our future work aims to expand into a multi-stage multi-timeframe model. This would differentiate the decision intervals for day-ahead and real-time markets, as discussed in [12]. Furthermore, we plan to explore a dynamic, multi-stage approach in response to evolving uncertainties, as highlighted in [24]. These steps will build upon the current study's foundations, addressing its limitations and deepening our analysis.

Algorithm 1: Primal Decomposition of Problem (3).

while $\boldsymbol{\lambda}^w(\boldsymbol{y}) \neq \boldsymbol{\lambda}^x(\boldsymbol{y})$ **do**
  $\boldsymbol{y} \leftarrow \boldsymbol{y} - \alpha(\boldsymbol{\lambda}^w(\boldsymbol{y}) - \boldsymbol{\lambda}^x(\boldsymbol{y}))$;
  Solve Problem (14) to find an optimal $\boldsymbol{w}$ and $\boldsymbol{\lambda}^w(\boldsymbol{y})$;
  Solve Problem (15) to find an optimal $\boldsymbol{x}$ and $\boldsymbol{\lambda}^x(\boldsymbol{y})$;
end while

APPENDIX A
PROOF OF PROPOSITION 1

We introduce a variable y_t (with a vector form of $\boldsymbol{y}$) to represent a general way of decomposing Constraint (3b) to decouple the decision variables $\boldsymbol{x}$ and $\boldsymbol{w}$ into Constraints (14b) and (15b). These two constraints are incorporated into the two sub-problems, separately, i.e., (14) and (15):

$$\max_{\boldsymbol{w}} \ \boldsymbol{p}^\dagger \boldsymbol{w} \tag{14a}$$

$$s.t. \quad w_t = \bar{w}_t - w^c_t + y_t, \ \forall t. := \lambda^w_t(y_t) \tag{14b}$$

$$0 \leq w^c_t \leq \bar{w}_t, \ \forall t. \tag{14c}$$

and

$$\max_{\mathbf{x}} \ \boldsymbol{p}^\dagger \boldsymbol{x} \tag{15a}$$

$$s.t. \quad x_t = d_t - c_t - y_t, \ \forall t, := \lambda^w_t(y_t) \tag{15b}$$

$$\text{Constraints}(2\text{c}) - (2\text{e}). \tag{15c}$$

Therefore, the aim of the master problem (3) is to maximize over the variable y_t. Let $\lambda^w_t(y_t)$ be the optimal dual variable associated with Constraint (14b) in Problem (14) with a vector form of $\boldsymbol{\lambda}^w(\boldsymbol{y})$. By definition of dual variables, the sub-gradient of Π^*_{RES} at y_t is $\lambda^w_t(y_t)$. Similarly, let $\lambda^x_t(y_t)$ be an optimal dual variable associated with Constraint (15b) in Problem (15) (with a vector form of $\boldsymbol{\lambda}^x(\boldsymbol{y})$) and the sub-gradient of Π^*_{Storage} at y_t is $-\lambda^x_t(y_t)$. Primal decomposition is solved by a sub-gradient master algorithm [35], which is simplified in Algorithm 1 and α is a step-size for updating $\boldsymbol{y}$.

When $\boldsymbol{\lambda}^w(\boldsymbol{y}) = \boldsymbol{\lambda}^x(\boldsymbol{y})$, Problem (3) reaches optimality.

On the other hand, by the Karush-Kuhn-Tucker (KKT) condition of each sub-problem, $\boldsymbol{\lambda}^w(\boldsymbol{y}) = \boldsymbol{\lambda}^x(\boldsymbol{y}) = \boldsymbol{p}$. Therefore, the optimality of the two sub-problems is the optimality of the original problem no matter what the value of $\boldsymbol{y}$ takes, which then implies Proposition 1, i.e., $\Pi^*_{\text{Joint}} = \Pi^*_{\text{RES}} + \Pi^*_{\text{Storage}}$ when $\boldsymbol{y} = \mathbf{0}$.

APPENDIX B
PROOF FOR NON-SIMULTANEOUS CHARGING AND DISCHARGING

We leverage the KKT conditions to (3), the feasible points at which the storage system is simultaneously charging and discharging, are suboptimal when $p > 0$. This finding aligns with the results presented in [36]. Initially, we modify the constraints to the form presented in Equation (16). Subsequently, we examine the Lagrangian multipliers linked with each constraint to elucidate this result.

$$\max_{\boldsymbol{w},\boldsymbol{x}} \ \boldsymbol{p}^\dagger (\boldsymbol{x} + \boldsymbol{w})$$

$$
\begin{aligned}
s.t.\ & x_t + w_t = \bar{w}_t - w_t^c + d_t - c_t, := \mu_t,\ \forall t,\\
& 0 \le w_t^c \le \bar{w}_t, := \underline{\lambda}_{\text{cur}}^t, \bar{\lambda}_{\text{cur}}^t,\ \forall t,\\
& 0 \le d_t \le L, := \underline{\lambda}_{\text{dis}}^t, \bar{\lambda}_{\text{dis}}^t,\ \forall t,\\
& 0 \le c_t \le L, := \underline{\lambda}_{\text{ch}}^t, \bar{\lambda}_{\text{ch}}^t,\ \forall t,\\
& -S_0 + \sum\nolimits_{n=1}^{t} (1/\eta_d d_t - \eta_c c_t) \le 0, := \underline{\lambda}_{\text{soc}}^t,\ \forall t,\\
& S_0 + \sum\nolimits_{n=1}^{t} (\eta_c c_t - 1/\eta_d d_t) - \bar{S} \le 0 := \bar{\lambda}_{\text{soc}}^t, \forall t. \quad (16)
\end{aligned}
$$

The stationary KKT condition at the optimal points should satisfy (17).

$$p_t - \mu_t = 0, \quad (17a)$$

$$\underline{\lambda}_{\text{ch}}^t + \bar{\lambda}_{\text{ch}}^t + \eta_c \sum\nolimits_{n=t}^{N} (\bar{\lambda}_{\text{soc}}^n - \underline{\lambda}_{\text{soc}}^n) + \mu_t = 0, \quad (17b)$$

$$\underline{\lambda}_{\text{dis}}^t + \bar{\lambda}_{\text{dis}}^t + 1/\eta_d \sum\nolimits_{n=t}^{N} (\underline{\lambda}_{\text{soc}}^n - \bar{\lambda}_{\text{soc}}^n) - \mu_t = 0, \quad (17c)$$

$$-\underline{\lambda}_{\text{cur}}^t + \bar{\lambda}_{\text{cur}}^t + \mu_t = 0. \quad (17d)$$

If we combine (17c) and (17d), we have:

$$\underline{\lambda}_{\text{dis}}^t + \bar{\lambda}_{\text{dis}}^t + 1/(\eta_c\eta_d)(\underline{\lambda}_{\text{ch}}^t + \bar{\lambda}_{\text{ch}}^t) + (1/(\eta_c\eta_d) - 1)\mu_t = 0. \quad (18)$$

Due to the complementary slackness condition, if $c_t > 0$ and $d_t > 0$ at the same time, $\underline{\lambda}_{\text{dis}}^t = \underline{\lambda}_{\text{ch}}^t = 0$ holds. The dual feasibility condition requires $\bar{\lambda}_{\text{dis}}^t = \bar{\lambda}_{\text{ch}}^t \ge 0$. Moreover, if $p_t > 0$, we have $\mu_t > 0$ due to (17a). This scenario contradicts (18) and thus the KKT condition does not hold. Therefore, simultaneous charging and discharging are suboptimal in our formulation (3) when $p_t > 0, \forall t$.

Appendix C
Proof of Proposition 3

Initially, we assume that the distributions of the uncertainty factors are discrete so that the optimization can be extended to a finite number of scenarios. We extend Problem (4) as an example, which can be written as:

$$\max\nolimits_{\boldsymbol{w}^{\mathbf{D}}, \boldsymbol{w}^{\mathbf{R}}}\ \boldsymbol{p}^{\mathbf{D}\dagger}\boldsymbol{w}^D + \sum\nolimits_{i\in\mathcal{I}} \pi_i \widetilde{\mathbf{p}}_i^{\mathbf{R}\dagger} \boldsymbol{w}_i^{\mathbf{R}} \quad (19a)$$

$$s.t.\ (\text{DA})\ \ w_t^D \geqslant 0,\ \forall t, \quad (19b)$$

$$(\text{RT}-i)\ \ w_t^D + w_{t,i}^R = \widetilde{w}_{t,i} - w_{t,i}^c,\ \forall t,\ := \lambda_{t,i}^w \quad (19c)$$

$$0 \le w_{t,i}^c \le \widetilde{w}_{t,i},\ \forall t. \quad (19d)$$

where $\mathcal{I}$ represents the set of scenarios and π_i denotes the probability of scenario i. In the i-th scenario, the real-time price is denoted as $\widetilde{\mathbf{p}}_i^{\mathbf{R}\dagger}$ the actual RES power output is $\widetilde{w}_{t,i}$, the real-time recourse decision of the RES generator is $w_{t,i}^R$. The counterpart of Constraint (19c) for Problem (6) and (8) are Constraints (20) and (21), respectively.

$$(\text{RT}-i)\quad x_t^D + x_{t,i}^R = d_{t,i}^F - c_{t,i}^F,\ := \lambda_{t,i}^x. \quad (20)$$

$$(\text{RT}-i)\ \ w_t^D + x_t^D + x_{t,i}^R + w_{t,i}^R = d_{t,i}^F - c_{t,i}^F + \widetilde{w}_{t,i} - w_{t,i}^c. \quad (21)$$

Constraints (19c) and (20) can be regarded as a way of decomposing Constraint (21) to decouple $x_{t,i}^R$ and $w_{t,i}^R$. Therefore, the extended formulation of Problem (8) can be regarded as a master problem, and the extended formulation of Problems (4) and (6) are two sub-problems. Similar to the proof in Appendix A, the optimality of the two sub-problems is the optimality of the original problem since the Lagrangian variables related to Constraint (19c) and (20) satisfy $\lambda_{t,i}^w = \lambda_{t,i}^x = \pi_i p_{t,i}^R$.

When dealing with continuous distributions of uncertain factors, an extensive formulation based on finite scenarios can only represent the empirical distributions. However, the Law of Large Numbers assures that as the number of scenarios increases, the empirical distributions will converge to the true underlying distribution. This convergence ensures the reliability of the scenario-based formulation, thus maintaining the validity of Proposition 3 (Chap. 5 of [37]).

Appendix D
Details of Example 2

As for the energy storage operation in the disjoint operation mode, Constraints (6b)–(6e) naturally lead to $x_1^D = -x_2^D$ and Constraints (7b)–(7d) lead to $x_1^R = -x_2^R$. The optimization problem (6) can be reformulated as:

$$
\begin{aligned}
&\max_{x_1^D} \left(p_1^D - p_2^D\right)\ x_1^D + \min\nolimits_{p_1^R, p_2^R} \max\nolimits_{x_1^R} \left(p_1^R - p_2^R\right)\ x_1^R\\
&s.t.\ -5 \le x_1^D \le 5, -5 \le x_1^D + x_1^R \le 5.
\end{aligned}
$$

Since x_1^R depends on p_1^R and p_2^R, if $p_1^R > p_2^R$, x_1^R can only be non-positive (≤ 0). Conversely, if $p_1^R < p_2^R$, x_1^R can only be non-negative (≥ 0). Both cases can result in a non-negative profit in real time. Hence, the worst scenario for real-time prices is $p_1^{R^*} = p_2^{R^*}$, and the optimal strategy for the energy storage owner is $x_1^D = -5$ and $x_2^D = 5$.

As for the joint operation mode, if we denote $z_t = d_t^F - c_t^F$, Constraint (8d) leads to $x_1^D = -x_2^D$ and Constraint (9c) leads to $z_1 = -z_2$. Hence, the optimization problem (8) can be formulated as:

$$
\begin{aligned}
&\max\nolimits_{x_1^D, w_1^D, w_2^D} \left[\left(p_1^D - p_2^D\right) x_1^D + p_1^D w_1^D + p_2^D w_2^D\right]\\
&+ \min\nolimits_{\widetilde{p}_1^R, \widetilde{p}_2^R, \widetilde{w}_1, \widetilde{w}_2} \max\nolimits_{z_1} \left[\widetilde{p}_1^R \left(\widetilde{w}_1 + z_1 - w_1^D - x_1^D\right)\right.\\
&\left. + \widetilde{p}_2^R \left(\widetilde{w}_2 - z_1 - w_2^D + x_2^D\right)\right]\\
&s.t. -5 \le x_1^D \le 5\ -5 \le z_1 \le 5,\\
&w_1^D > 0, w_2^D > 0.
\end{aligned}
$$

As can be found in the objective function, the worst scenario for RES output is $\widetilde{w}_1^* = 15, \widetilde{w}_2^* = 1$. Next, we show the worst scenario of real-time price. Given that $p_1^D < \widetilde{p}_1^R$ and $p_2^D < \widetilde{p}_2^R$ hold for all values in the uncertainty set, it follows that $x_1^D = x_2^D = 0$. Hence, for each unit increase in $\widetilde{p}_1^R$, the objective function increases by $\widetilde{w}_1 + z_1 - x_1^D \ge 15 - 5 - 5 > 0$. This implies that the worst-case scenario for the real-time price at time period 1 is $\widetilde{p}_1^{R*} = 25$. Similarly, for each unit increase in $\widetilde{p}_2^R$, the objective function increases by $\widetilde{w}_2 + z_2 - x_2^D \ge 20 - 5 - 5 > 0$. This

implies that the worst-case scenario for the real-time price at time period 1 is $\widetilde{p}_1^{R*} = 35$.

Appendix E
Proof of Proposition 5

Similar to the proof of Proposition 2, the combination of Problem (4) and Problem (6) has a more restricted feasible space compared to Problem (8). Meanwhile, for each solution pair within the feasible space, w_t^R and x_t^R, the sum of the values of the objective functions of Problem (4) and Problem (6) is no larger than that of Problem (8):

$$\widetilde{p}_t^R(w_t^R + x_t^R)\begin{cases} = \widetilde{p}_t^R w_t^R + \widetilde{p}_t^R x_t^R, & w_t^R x_t^R > 0, \\ > \widetilde{p}_t^R w_t^R + \widetilde{p}_t^R x_t^R, & w_t^R x_t^R < 0. \end{cases}$$

Therefore, it is straightforward that $\Pi^*_{\text{Joint}} - \Pi^*_{\text{ORI}} = \Pi^*_{\text{Joint}} - \Pi^*_{\text{RES}} \geq \Pi^*_{\text{Storage}}$.

Appendix F
Ancillary Service Formulation

The storage arbitrageur's multi-timeframe optimization, incorporating AS products, can be formulated as in (22).

$$\begin{aligned} \max_{\boldsymbol{x^D}, \boldsymbol{r^U}, \boldsymbol{r^L}} \ & \boldsymbol{p^{D\dagger}} \boldsymbol{x^D} + \boldsymbol{p^{U\dagger}} \boldsymbol{r^U} + \boldsymbol{p^{L\dagger}} \boldsymbol{r^L} \\ & + \boldsymbol{\rho} \left[\max_{\boldsymbol{x^R} \in \Omega^X(\boldsymbol{x^D}, \boldsymbol{r^U}, \boldsymbol{r^L}, \widetilde{\mathbf{p}}^{\mathbf{R}}, \widetilde{\boldsymbol{\tau}}^{\mathbf{U}}, \widetilde{\boldsymbol{\tau}}^{\mathbf{L}})} \widetilde{\mathbf{p}}^{\mathbf{R}\dagger} \boldsymbol{x^R} \right] \\ s.t. \ & \text{Constraint (6b)} - \text{(6d)}, \\ & \text{Constraint (12)}. \end{aligned} \tag{22}$$

The feasible region of x_t^R can be defined in (23).

$$\begin{aligned} & \Omega_t^X(x_t^D, r_t^U, r_t^D, \widetilde{p}_t^R, \{\widetilde{\tau}_{t,k}^U, \widetilde{\tau}_{t,k}^L\}_{k=1,\dots,K}) \\ & := \{ \text{ Constraint (13)}, \\ & \text{Constraint (7d)} \}. \end{aligned} \tag{23}$$

The multi-timeframe optimization for joint operation, incorporating AS products, can be formulated as in (24).

$$\begin{aligned} \max_{\boldsymbol{x^D}, \boldsymbol{w^D}, \boldsymbol{r^U}, \boldsymbol{r^L}} \ & \boldsymbol{p^{D\dagger}} \left(\boldsymbol{x^D} + \boldsymbol{w^D} \right) + \boldsymbol{p^{U\dagger}} \boldsymbol{r^U} + \boldsymbol{p^{L\dagger}} \boldsymbol{r^L} \\ & + \boldsymbol{\rho} \left[\max_{(\boldsymbol{x^R}, \boldsymbol{w^R}) \in \Omega^J(\substack{\boldsymbol{x^D}, \boldsymbol{w^D}, \boldsymbol{r^U}, \boldsymbol{r^L}, \\ \widetilde{\mathbf{p}}^{\mathbf{R}}, \widetilde{\boldsymbol{\tau}}^{\mathbf{U}}, \widetilde{\boldsymbol{\tau}}^{\mathbf{L}}, \widetilde{\boldsymbol{w}}})} \widetilde{\mathbf{p}}^{\mathbf{R}\dagger} \left(\boldsymbol{x^R} + \boldsymbol{w^R} \right) \right] \\ s.t. \ & \text{Constraint (4b)}, \\ & \text{Constraints (6b)} - \text{(6d)}, \\ & \text{Constraint (12)}. \end{aligned} \tag{24}$$

The feasible region of w_t^R and x_t^R can be defined in (25).

$$\begin{aligned} & \Omega_t^J(x_t^D, w_t^D, r_t^U, r_t^D, \widetilde{p}_t^R, \{\widetilde{\tau}_{t,k}^U, \widetilde{\tau}_{t,k}^L\}_{k=1,\dots,K}) \\ & := \{ \quad x_t^D + w_t^D + x_t^R + w_t^R + \widetilde{\tau}_{t,k}^U r_t^U - \widetilde{\tau}_{t,k}^L r_t^L \\ & = \widetilde{w}_t - w_t^c + d_{t,k}^F - c_{t,k}^F, \ \forall t, \forall k, \\ & \text{Constraint (5b)}, \\ & \text{Constraints (13b)} - \text{(13c)}, \\ & \text{Constraint (7d)} \}. \end{aligned} \tag{25a}$$

Due to the variability and uncertainty, the disjoint RES generator is excluded from regulation markets, retaining its operation as specified in Problem (4). Following the approach in Appendix C, the extended formulation of Constraints (5a) and (13a) can be regarded as a way of decomposing Constraint (25a). Moreover, when agents are all price-takers, for each realized scenario, the Lagrangian variables related to Constraint (5a) and Constraint (13a) are identical. Consequently, the profits of joint and disjoint operations are equal, resulting in an identical value of storage for the RES and the arbitrageur.

Appendix G
Formulation of Deterministic Real-Time Operation in Out-of-Sample Analysis

Denote the optimal day-ahead decisions by $w^D_{*,\text{joint}}$ and $x^D_{*,\text{joint}}$ for the joint problem, $w^D_{*,\text{RES}}$ for the RES optimization and $x^D_{*,\text{Arb}}$ for the storage optimization. For sample number i, the deterministic real-time problem for RES is Problem (26).

$$\begin{aligned} \max_{\boldsymbol{w}_i^{\mathbf{R}}} \ & \boldsymbol{p^{D\dagger}} \boldsymbol{w}^D_{*,\text{RES}} + \widetilde{\mathbf{p}}_{\mathbf{i}}^{\mathbf{R}\dagger} \boldsymbol{w}_i^{\mathbf{R}} \\ s.t. \ & \text{Constraint (5a)} - \text{(5b)}. \end{aligned} \tag{26}$$

The deterministic real-time problem for RES is Problem (27).

$$\begin{aligned} \max_{\boldsymbol{x}_i^{\mathbf{R}}} \ & \boldsymbol{p^{D\dagger}} \boldsymbol{x}^{\boldsymbol{D}}_{*,\text{Arb}} + \widetilde{\mathbf{p}}_i^{\mathbf{R}\dagger} \boldsymbol{x}_i^{\mathbf{R}} \\ s.t. \ & \text{Constraint (7a)} - \text{(7d)}. \end{aligned} \tag{27}$$

The deterministic real-time problem for joint operation is Problem (28).

$$\begin{aligned} \max_{\boldsymbol{w}_i^{\mathbf{R}}, \boldsymbol{x}_i^{\mathbf{R}}} \ & \boldsymbol{p}^{\mathbf{D}^\dagger} \left(\boldsymbol{w}^{\mathbf{D}}_{*,\text{joint}} + \mathbf{x}^{\mathbf{D}}_{*,\text{joint}} \right) + \widetilde{\mathbf{p}}_i^{\mathbf{R}\dagger} \left(\boldsymbol{w}_i^{\mathbf{R}} + \mathbf{x}_i^{\mathbf{R}} \right) \\ s.t. \ & \text{Constraint (9a)} - \text{(9c)}. \end{aligned} \tag{28}$$

References

[1] IEA, "How rapidly will the global electricity storage market grow by 2026," Int. Energy Agency, Paris, Tech. Rep., 2021. [Online]. Available: https://www.iea.org/articles/how-rapidly-will-the-global-electricity-storage-market-grow-by-2026

[2] R. Joseph et al., "Queued up: Characteristics of power plants seeking transmission interconnection as of the end of 2022," Lawrence Berkeley Nat. Lab., Berkeley, CA, USA, Tech. Rep., 2023. [Online]. Available: https://emp.lbl.gov/queues

[3] J. Barton and D. Infield, "Energy storage and its use with intermittent renewable energy," *IEEE Trans. Energy Convers.*, vol. 19, no. 2, pp. 441–448, Jun. 2004.

[4] G. N. Bathurst and G. Strbac, "Value of combining energy storage and wind in short-term energy and balancing markets," *Elect. Power Syst. Res.*, vol. 67, no. 1, pp. 1–8, 2003.

[5] R. Sioshansi, "Increasing the value of wind with energy storage," *Energy J.*, vol. 32, no. 2, pp. 1–30, 2011.

[6] H. Ding, P. Pinson, Z. Hu, J. Wang, and Y. Song, "Optimal offering and operating strategy for a large wind-storage system as a price maker," *IEEE Trans. Power Syst.*, vol. 32, no. 6, pp. 4904–4913, Nov. 2017.

[7] M. E. Khodayar and M. Shahidehpour, "Stochastic price-based coordination of intrahour wind energy and storage in a generation company," *IEEE Trans. Sustain. Energy*, vol. 4, no. 3, pp. 554–562, Jul. 2013.
[8] H. Ding, Z. Hu, and Y. Song, "Rolling optimization of wind farm and energy storage system in electricity markets," *IEEE Trans. Power Syst.*, vol. 30, no. 5, pp. 2676–2684, Sep. 2015.
[9] J. H. Kim and W. B. Powell, "Optimal energy commitments with storage and intermittent supply," *Operations Res.*, vol. 59, no. 6, pp. 1347–1360, 2011.
[10] R. Jiang, J. Wang, and Y. Guan, "Robust unit commitment with wind power and pumped storage hydro," *IEEE Trans. Power Syst.*, vol. 27, no. 2, pp. 800–810, May 2012.
[11] U. Yıldıran and İ. Kayahan, "Risk-averse stochastic model predictive control-based real-time operation method for a wind energy generation system supported by a pumped hydro storage unit," *Appl. Energy*, vol. 226, pp. 631–643, 2018.
[12] T. Ochoa, E. Gil, A. Angulo, and C. Valle, "Multi-agent deep reinforcement learning for efficient multi-timescale bidding of a hybrid power plant in day-ahead and real-time markets," *Appl. Energy*, vol. 317, 2022, Art. no. 119067.
[13] C. Pan, H. Fan, R. Zhang, J. Sun, Y. Wang, and Y. Sun, "An improved multi-timescale coordinated control strategy for an integrated energy system with a hybrid energy storage system," *Appl. Energy*, vol. 343, 2023, Art. no. 121137.
[14] D. Zafirakis, K. J. Chalvatzis, G. Baiocchi, and G. Daskalakis, "The value of arbitrage for energy storage: Evidence from European electricity markets," *Appl. Energy*, vol. 184, pp. 971–986, 2016.
[15] H. Wang and B. Zhang, "Energy storage arbitrage in real-time markets via reinforcement learning," in *Proc. IEEE Power Energy Soc. Gen. Meeting*, 2018, pp. 1–5.
[16] D. Krishnamurthy, C. Uckun, Z. Zhou, P. R. Thimmapuram, and A. Botterud, "Energy storage arbitrage under day-ahead and real-time price uncertainty," *IEEE Trans. Power Syst.*, vol. 33, no. 1, pp. 84–93, Jan. 2018.
[17] N. Löhndorf and D. Wozabal, "The value of coordination in multimarket bidding of grid energy storage," *Operations Res.*, vol. 71, no. 1, pp. 1–22, 2023.
[18] G. Terça and D. Wozabal, "Economies of scope for electricity storage and variable renewables," *IEEE Trans. Power Syst.*, vol. 36, no. 2, pp. 1328–1337, Mar. 2021.
[19] M. Zheng, C. J. Meinrenken, and K. S. Lackner, "Smart households: Dispatch strategies and economic analysis of distributed energy storage for residential peak shaving," *Appl. Energy*, vol. 147, pp. 246–257, 2015.
[20] Y. Shi, B. Xu, D. Wang, and B. Zhang, "Using battery storage for peak shaving and frequency regulation: Joint optimization for superlinear gains," *IEEE Trans. Power Syst.*, vol. 33, no. 3, pp. 2882–2894, May 2018.
[21] A. K. Varkani, A. Daraeepour, and H. Monsef, "A new self-scheduling strategy for integrated operation of wind and pumped-storage power plants in power markets," *Appl. Energy*, vol. 88, no. 12, pp. 5002–5012, 2011.
[22] A. J. Conejo, J. Contreras, J. M. Arroyo, and S. D. l. Torre, "Optimal response of an oligopolistic generating company to a competitive pool-based electric power market," *IEEE Trans. Power Syst.*, vol. 17, no. 2, pp. 424–430, May 2002.
[23] N. Lacey, *The Prisoners' Dilemma: Political Economy and Punishment in Contemporary Democracies. The Hamlyn Lectures*. Cambridge, U.K.: Cambridge Univ. Press, 2008.
[24] N. Gu, J. Cui, and C. Wu, "An auto-tuned robust dispatch strategy for virtual power plants to provide multi-stage real-time balancing service," *IEEE Trans. Smart Grid*, vol. 14, no. 6, pp. 4494–4507, Nov. 2023.
[25] R. T. Rockafellar, "Coherent approaches to risk in optimization under uncertainty," in *OR Tools and Applications: Glimpses of Future Technologies*. Catonsville, MD, USA: Informs, 2007, pp. 38–61.
[26] J. Cui, N. Gu, T. Zhao, C. Wu, and M. Chen, "Forecast competition in energy imbalance market," *IEEE Trans. Power Syst.*, vol. 37, no. 3, pp. 2397–2413, May 2022.
[27] J. M. Kemp, D. Millstein, J. H. Kim, and R. Wiser, "Interactions between hybrid power plant development and local transmission in congested regions," *Adv. Appl. Energy*, vol. 10, 2023, Art. no. 100133.
[28] M. Grant and S. Boyd, "Graph implementations for nonsmooth convex programs," *Recent Adv. Learn. Control*, V. Blondel, S. Boyd, H. Kimura, S. Boyd, and H. Kimura, Lecture Notes in Control and Information Sciences, 2008, pp. 95–110. [Online]. Available: http://stanford.edu/~boyd/graph_dcp.html
[29] R. Joshua, "The impact of renewables in ercot." 2023. Accessed: May 20, 2023. [Online]. Available: https://www.ideasmiths.net/wp-content/uploads/2023/05/Impact-of-Renewables-in-ERCOT_FINAL.pdf
[30] ERCOT, "Hourly load data archives." 2023. Accessed: May 20, 2023. [Online]. Available: https://www.ercot.com/gridinfo/load/load_hist
[31] ERCOT, "Hourly aggregated wind and solar output." 2023. Accessed: May 20, 2023. [Online]. Available: https://www.ercot.com/mp/data-products/data-product-details?id=PG7-126-M
[32] ERCOT, "Ercot market prices." 2023. Accessed: May 20, 2023. [Online]. Available: https://www.ercot.com/mktinfo/prices
[33] N. Gu, H. Wang, J. Zhang, and C. Wu, "Bridging chance-constrained and robust optimization in an emission-aware economic dispatch with energy storage," *IEEE Trans. Power Syst.*, vol. 37, no. 2, pp. 1078–1090, Mar. 2022.
[34] A. Arrigo, C. Ordoudis, J. Kazempour, Z. D. Grève, J.-F. Toubeau, and F. Vallée, "Optimal power flow under uncertainty: An extensive out-of-sample analysis," in *Proc. IEEE PES Innov. Smart Grid Technol. Eur.*, 2019, pp. 1–5.
[35] S. Boyd, L. Xiao, A. Mutapcic, and J. Mattingley, "Notes on decomposition methods," Stanford Univ., Stanford, CA, USA, Tech. Rep., 2008. [Online]. Available: https://see.stanford.edu/materials/lsocoee364b/08-decomposition_notes.pdf
[36] K. Garifi, K. Baker, D. Christensen, and B. Touri, "Control of energy storage in home energy management systems: Non-simultaneous charging and discharging guarantees," 2018*arXiv:1805.00100*.
[37] A. Shapiro, D. Dentcheva, and A. Ruszczynski, *Lectures on Stochastic Programming: Modeling and Theory*. Philadelphia, PA, USA: SIAM, 2021.

Nan Gu (Graduate Student Member, IEEE) received the bachelor's degree from the Department of Electrical Engineering, Tsinghua University, Beijing, China. She is currently working toward the Ph.D. degree with IIIS, Tsinghua University, advised by Professor Chenye Wu. She was awarded Excellent Graduate of Tsinghua University in 2019. Her research interests include optimal operation and market design of power systems.

Chenye Wu (Senior Member, IEEE) received the Ph.D. degree in computer science and technology at Institute for Interdisciplinary Information Sciences (IIIS), Tsinghua University, Beijing, China, in 2013. He is currently an Assistant Professor and the Presidential Young Fellow with the School of Science and Engineering, The Chinese University of Hong Kong, Shenzhen, Shenzhen, China. Before joining The Chinese University of Hong Kong Shenzhen, he was an Assistant Professor with IIIS, Tsinghua University. He worked with ETH Zurich, Zürich, Switzerland, as a Research Scientist, working with Professor Gabriela Hug, in 2016. Before that, Prof. Kameshwar Poolla and Prof. Pravin Varaiya hosted Dr. Wu as a Postdoctoral Researcher with University of California, Berkeley, Berkeley, CA, USA, for two years. During 2013–2014, he spent one year with Carnegie Mellon University, Pittsburgh, PA, USA, as a Postdoc Fellow, hosted by Prof. Gabriela Hug and Prof. Soummya Kar. He is currently working on economic analysis, optimal control and operation of power systems. His Ph.D. Advisor is Professor Andrew Yao, the laureate of the A.M. Turing Award in the year of 2000. Dr. Wu was the co-recipients of IEEE SmartGridComm 2012 Best Paper Award, IEEE PES General Meeting 2013 Best Paper Award, IEEE PES General Meeting 2020 Best Paper Award.

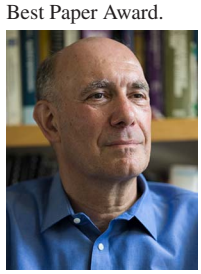

Daniel S. Kirschen (Fellow, IEEE) received the Electro-Mechanical Engineering degree from the Free University of Brussels, Belgium, and the Ph.D. degree from the University of Wisconsin-Madison, Madison, WI, USA. He is currently the Donald W. and Ruth Mary Close Professor of electrical and computer engineering with the University of Washington, Seattle, WA, USA. He is the author of three books and more than 200 scientific papers. His research interests include the integration of renewable energy sources in the grid, power system economics and power system resilience. Prior to joining the University of Washington, he taught for 16 years with The University of Manchester, Manchester, U.K. Before becoming an academic, he worked for Control Data and Siemens on the development of application software for utility control centers. He is the founding Editor-in-Chief of IEEE TRANSACTIONS ON ENERGY MARKETS, POLICY, AND REGULATION.